Colloids and Surfaces B: Biointerfaces 207 (2021) 111995

Contents lists available at ScienceDirect

Colloids and Surfaces B: Biointerfaces

journal homepage: www.elsevier.com/locate/colsurfb

Rapid synthesis of microwave-assisted zinc oxide nanorods on a paper-based analytical device for fluorometric detection of L-dopa

Yu-Hsuan Lin, Yi-Chun Yeh *

Department of Chemistry, National Taiwan Normal University, Taipei, 11677, Taiwan

ARTICLE INFO

Keywords:
Microwave-assisted
ZnO nanorods
Paper-based
Fluorometric detection
L-dopa
Fluorescence enhancement

ABSTRACT

L-dopa is a catecholamine neurotransmitter used to treat Parkinson's disease. This paper presents a low-cost paper-based biosensor aimed at enhancing the convenience of monitoring L-dopa concentrations. ZnO nanorods (ZnO-NRs) were synthesized on papers in less than 90 min using a microwave-assisted hydrothermal method. The ZnO-NRs amplify green fluorescence signals to enhance the detection sensitivity of L-dopa, best measured at excitation/emission wavelengths of 475/537 nm. We systematically characterized the effect of reaction conditions on the corresponding fluorescence enhancements. The proposed ZnO NRs-paper biosensor presented a ~3-fold increase in green fluorescence compared to unmodified papers. The linear range of detection for L-dopa was 25–2000 nM, with a limit of detection of 24 nM, which meets the clinical requirements for the monitoring of L-dopa in Parkinson's patients.

1. Introduction

ZnO nanomaterials have attracted tremendous attention for their unique optical properties, including a wide bandgap (approximately 3.37 eV at room temperature) and a large exciton binding energy (60 meV). The fact that ZnO nanomaterials are biocompatible [1], inexpensive [2], environmentally benign makes them a promising material for biomedical application [3,4]. They have also been formed into a variety of nanostructure morphologies, such as nanoparticles [5–7], nanowires [8–10], nanorods [11–13], and nano-flowers [14–16]. Specially, one-dimensional (1D) ZnO nanostructures array show significantly fluorescence enhancement properties in previous report [14]. This was due the direct fluorescence from the fluorophores as well as guided fluorescence from 1D ZnO nanostructures [14]. Many research groups fabricated not only ZnO but also metal/metal oxides on the surface of cellulose fiber for analytical and medical applications [17–19]. Notedly, the rapid microwave-assisted synthesis of nanomaterials on paper can be achieved at a relatively low reaction temperature at low cost [20,21].

L-dopa is a major precursor to produce dopamine through the enzyme aromatic L-amino acid decarboxylase. L-dopa is the medication most commonly prescribed for Parkinson's disease as an effective replacement for dopamine [22]. However, many studies have reported side-effects of this treatment, including orthostatic hypotension, excessive daytime somnolence, and nausea [23]. The closely monitoring of patients is crucial to making timely adjustments in L-dopa dosages [24]. L-dopa often coexists with other catecholamine analogs including dopamine, norepinephrine, and epinephrine [25]. A number of methods have been developed for quantification of L-dopa such as electrochemical sensors [26], high-performance liquid chromatography (HPLC) [27], sensors based on nanomaterials [28], and small-molecule fluorescence dyes [29]. The high sensitivity of electrochemical sensors renders then susceptible to acquaintance redox potentials. In cases where catecholamines coexist with urea and ascorbic acid, the peaks of catecholamines tend to overlap [30]. The high specificity of HPLC can only be achieved through the use of expensive equipment, highly-skilled operators, and complicated pretreatment procedures. Compared with other methods, nanomaterial-based fluorescent sensors provide a low detection limit and ease of visibility at low cost [31–33].

In previous study, we developed a colorimetric L-dopa biosensor based on the formation of betalamic acid by L-dopa 4,5-dioxygenase and further non-enzymatic condensation with amines to form betaxanthins [34]. Glu-betaxanthins (Glu-BX) presented strong green fluorescence for the determination of L-dopa at a linear range of 5–500 μM. However, the in vivo detection of L-dopa was limited by ultralow concentrations, rapid oxidation, and physiological interference. In the current study, we combined the advantages of fluorescent sensors with those of nanomaterials. ZnO-NRs were prepared on filter paper via

* Corresponding author.
E-mail address: yichuny@ntnu.edu.tw (Y.-C. Yeh).

https://doi.org/10.1016/j.colsurfb.2021.111995
Received 5 June 2021; Received in revised form 14 July 2021; Accepted 18 July 2021
Available online 19 July 2021

microwave-assisted hydrothermal synthesis under various synthesis conditions. The resulting ZnO-NRs were shown to amplify the green fluorescence signalfrom Glu-BX to facilitate the detection of L-dopa [35]. The green fluorescence signal from the proposed ZnO NRs-paper biosensor was a ~3-fold higher than that of non-modified paper, with a L-dopa detection limit of 24 nM. The proposed ZnO NRs-paper was successfully applied to the detection of L-dopa in physiological bio-fluids, including fetal bovine serum (FBS) and artificial urine (AU). The proposed ZnO NRs-paper enabled the quantitative analysis of L-dopa on a complex matrix quickly and easily.

2. Materials and methods

2.1. Chemicals

Dopamine (DA), L-dopa, tyramine, ascorbic acid (AA), norepinephrine (NE), epinephrine (Epi), glutamic acid, and phenylalanine (Phe) were purchased from ACROS. Iron(II) sulfate, tryptophan, phenylethylamine (PEA) were purchased from Sigma-Aldrich. Glycine, isopropyl β-D-1-thiogalactopyranoside (IPTG), carbenicillin and glycerol were purchased from Amresco. Tyrosine was purchased from KYOWA and Merck. FBS and AU were purchased from GE Healthcare Life Sciences. Calcium chloride was purchased from Ferak Berlin GmbH. Magnesium sulfate was purchased from Fisher chemical.

2.2. Synthesis of ZnO NRs on chromatography paper

The ZnO-NRs were prepared from solutions of zinc nitrate hexahydrate and hexamethylenetetramine on the Whatman No. 93 chromatography paper with a seed layer prepared from immersed in zinc acetate solution (2.19 g/100 mL water) for 1 min and followed by heating at 100 °C for 1 h. The chromatography paper with seeding layer was immersed in the solution containing 1.022 mol/L ammonia hydroxide, 110 mmol/L zinc nitrate hexahydrate, 64.4 mmol/L hexamethylenetetramine, and 4 mg/mL polyethyleneimine. ZnO-NRs were synthesized by conventional and microwave-assisted hydrothermal methods. For the hydrothermal synthesized ZnO-NRs, the resulting suspension solution was transferred into a teflon-lined stainless-steel autoclave and sealed tightly at 90 °C for 5 h in a furnace (Thermo scientific BF51828C-1). For the microwave-assisted hydrothermal synthesized ZnO-NRs, the resulting suspension solution were heated at 400 W for 90 min using a microwave digesting system (START D).

2.3. Detection of L-dopa by protein-based methods

4,5-Dioxygenase protein extractions were collected following standard protocol. The reaction medium containing 25 mM sodium phosphate buffer (pH 6.8), 0.25 mg/mL purified protein, 10 mM ascorbic acid, 0.5 mM iron(II) sulfate, and various concentrations of L-dopa (0, 25, 50, 250, 500, 1000, 1500, 2000 nM) were mixed. The mixtures were reacted at 37 °C for 30 min until a yellow solution was obtained. The solution was reacted with glutamic acid at room temperature for 16 h. The production of Glu-BX was synthesized by Schiff condensation. The Glu-BX synthesized by L-dopa of various concentrations was spotted on the ZnO NRs-paper. The green fluorescence was measured by FluorChem M (TCX-LS13) at excitation/emission wavelengths of 475/537 nm. The images were converted to grayscale value, and analyzed by ImageJ.

2.4. Interference study

The fluorescence was measured as described above in the presence of other amino acids, neurotransmitters, and structural analogs, such as DA, Epi, NE, PEA, tyramine, Phe, tyrosine, tryptophan, and AA at 2 μM. Measurements were performed at room temperature on ZnO-NRs-paper.

2.5. Bacteria growth conditions

The bacterial cells that express 4,5-Dioxygenase protein were transformed into *E. coli* BL21. The cells were diluted (1 %) in 6 mL LB medium and incubated for 7 h. After culturing for 7 h, the cells were diluted (0.1 %) in M9 medium. The M9 medium was supplemented with 5 mg/mL thiamine hydrochloride, 11.1 μg/mL calcium chloride, 0.24 mg/mL magnesium sulfate, and 1% glycerol. Both the LB and M9 medium were supplemented with 50 μg/mL of carbenicillin.

2.6. Detection of L-dopa by cell-based method

Cells were diluted in M9 medium and incubated at 250 rpm, 37 °C (~O.D.600 = 0.4). The cells were induced with 100 μM IPTG, 10 μM iron(II) sulfate, 10 mM ascorbic acid, and various concentrations of L-dopa (0, 25, 50, 250, 500, 1000, 1500, 2000 nM). The mixtures were reacted at 37 °C for 30 min to allow enzymatic conversion of L-dopa to betalamic acid. The addition of glutamic acid to a medium with betalamic acid leads to the production of Glu-BX by Schiff condensation. After 4 h, Glu-Bx was spotted on the ZnO NRs-paper and examined the green fluorescence intensity by FluorChem M (TCX-LS13) as described above.

2.7. Detection of L-dopa in real sample

AU and FBS were diluted (1:1, volume %) in cell-based medium before all measurements.

3. Results and discussion

3.1. SEM images and XRD characterization of ZnO-NRs on paper-based

We first examined morphological difference among ZnO-NRs prepared on paper using conventional hydrothermal methods and microwave-assisted methods. (Figs. S1A and S1C) present scanning electron microscope (SEM) images of ZnO-NRs synthesized using the two methods. The microwave-assisted and conventional hydrothermal methods produced both vertically-aligned ZnO-NRs with high-density coverage; however, the hydrothermal approach resulted in a long reaction time (5 h). We therefore adopted the microwave system to synthesize the ZnO-NRs for subsequent experiments. The X-ray powder diffraction (XRD) spectrum of as-prepared paper surface was characterized using an X-ray diffractometer to elucidate the chemical composition. The XRD spectrum of cellulose in the paper presented distinct peaks at 16.2°and 22.7° (Fig. S1D). Additional peaks were also observed at $2\theta = 31.9°$, 34.6°, 36.5°, 47.8°, and 56.8° (Fig. S1D) indicating that the crystallographic structure of the ZnO-NRs was the wurtzite (JCPDS file number 36-1451). The XRD spectrum of ZnO-NRs was nearly identical to those synthesized from hydrothermal approach (Fig. S1B). Transmission electron microscope (TEM) images of ZnO-NRs prepared from hydrothermal approach were shown in (Fig. S1E and F)

3.2. Signal enhancement by ZnO-NRs on paper of various porosities

Next, we compared the effects of ZnO-NRs in enhancing fluorescence to cellulose paper samples of various porosities. The surface morphologies of papers before the modification of ZnO-NRs were characterized by SEM. (Fig. S2A-2F) presents the SEM images of Whatman chromatography papers with pore sizes of 2.5, 10, and 25 μm without and with ZnO-NRs. We also examined the photos and intensity of green fluorescence of the same ZnO NR-papers after they were spotted with Glu-BX solutions synthesized by L-dopa of various concentrations. ZnO NRs have slight green fluorescence compared with bare cellulose paper which is consistent with previous study [36]. The protein buffer solution without L-dopa was used as a control (Blank). As shown in (Fig. S2G), the ZnO NRs-paper with the medium pore size presented the strongest

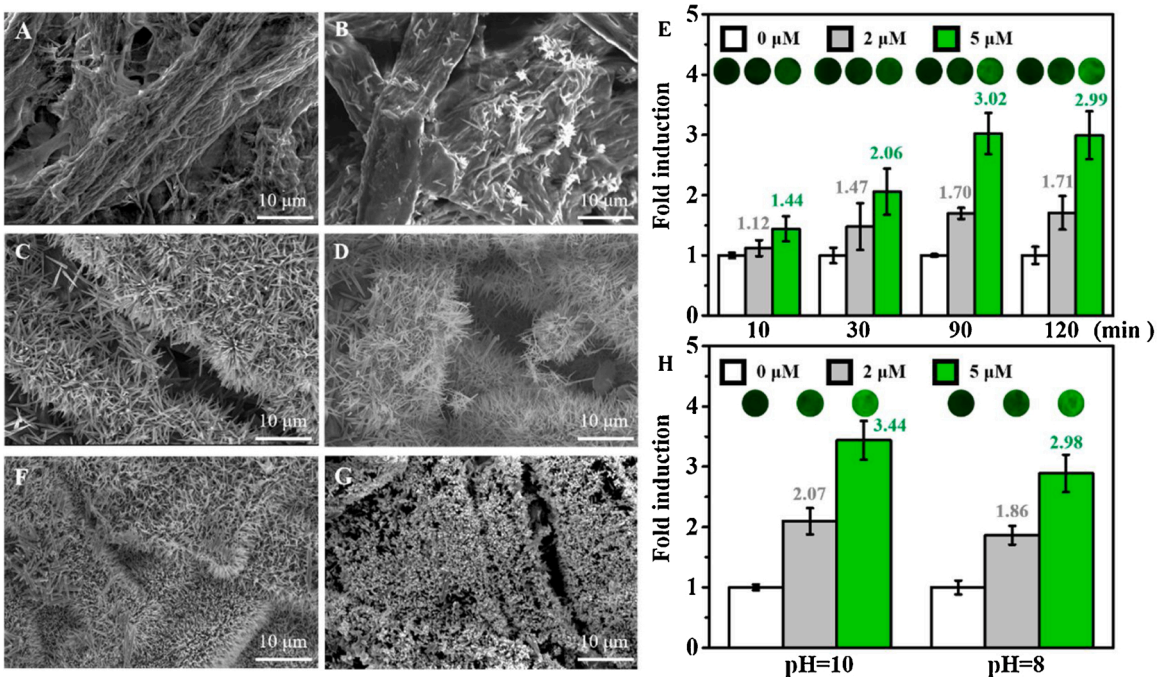

Fig. 1. SEM images of ZnO-NRs prepared by a microwave-assisted hydrothermal method with various reaction time including (A) 10, (B) 30, (C) 90, and (D) 120 min. (E) We characterized the effect of reaction time on its fluorescence enhancement (indicated by numbers). Glu-BX solutions synthesized by L-dopa at 0, 2, and 5 μM. Inset: the fluorescence images of ZnO-NRs/paper were acquired by using a fluorescence imager. Representative SEM images of ZnO-NRs synthesized at (F) pH = 10 and (G) pH = 8. (H) The effect of synthesis pH conditions on its fluorescence enhancement (indicated by numbers) of as-prepared ZnO NR/paper. Inset: the fluorescence images of ZnO-NRs papers were acquired by using a fluorescence imager.

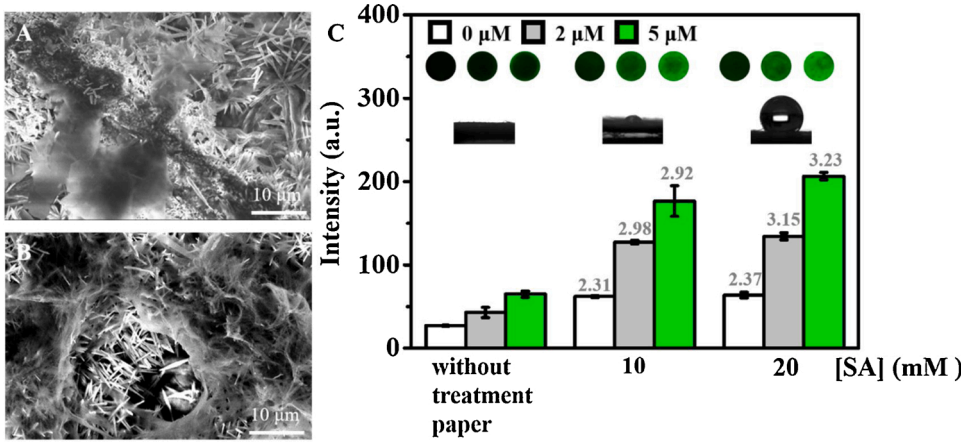

Fig. 2. SEM images of ZnO-NRs surface after treatment with (A) 10 mM and (B) 20 mM stearic acid. (C) The quantified enhancement intensities of ZnO NRs/paper after treatment with stearic acid at various concentrations (10 and 20 mM). Inset: contact angle of water and photo of green fluorescence images of ZnO-NR/paper. Glu-BX solutions which were synthesized by L-dopa of 0, 2, and 5 μM.

fluorescence enhancement. Thus, the paper with 10 μm pore was used for all subsequent tests. Additionally, the stability of as-prepared ZnO-NR-papers remain similarly after 3-month storage at room temperature (Fig. S2H).

3.3. Optimization of synthesis conditions for ZnO NRs-paper

We characterized the effect of reaction time on the final morphology of the ZnO NRs-paper and corresponding fluorescence enhancements. SEM images revealed that ZnO coverage increased with reaction time (Fig. 1A–D). Overall, the most pronounced fluorescence enhancement obtained at reaction times exceeding 90 min (Fig. 1E). We therefore adopted a 90 min microwave reaction time for following experiments. We also examined the effect of pH (between 10 and 8) on the morphology of ZnO-NRs (Fig. 1F and G). The most pronounced fluorescence enhancement was obtained under strongly basic conditions (Fig. 1H).

3.4. Surface modification of paper with stearic acid

The ZnO NRs-paper was also modified with the stearic acid, which is a low-cost and non-toxic long hydrophobic alkyl chain molecule. (Fig. 2) illustrates the signal enhancement and water contact angle before and after stearic acid modification. Prior to stearic acid treatment, the surface of the ZnO NRs-paper was hydrophilic. Following stearic acid treatment of 20 mM for 20 min, the surface of the ZnO NRs-paper had become hydrophobic, as indicated by the high water-contact-angle 130°, indicating a significant change in hydrophobicity. SEM revealed

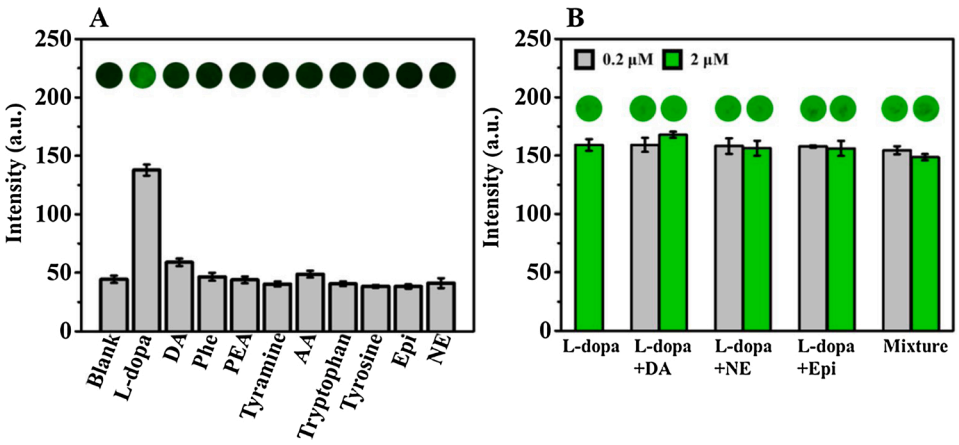

Fig. 3. (A) The selectivity of the 4,5-Dioxygenase protein in the presence of common interferences including DA, Phe, PEA, tyramine, AA, tryptophan, tyrosine, Epi, and NE at 2 μM was examined. The protein buffer solution without L-dopa was used as a control (Blank). Inset: the fluorescence images of ZnO-NRs/paper. (B) The green fluorescence intensities were compared in the presence of L-dopa alone, L-dopa with DA/NE/Epi, and a mixture of four. Two levels of concentrations were applied to each analyte respectively in the experiments (0.2 and 2 μM). Inset: the fluorescence images of ZnO-NRs papers.

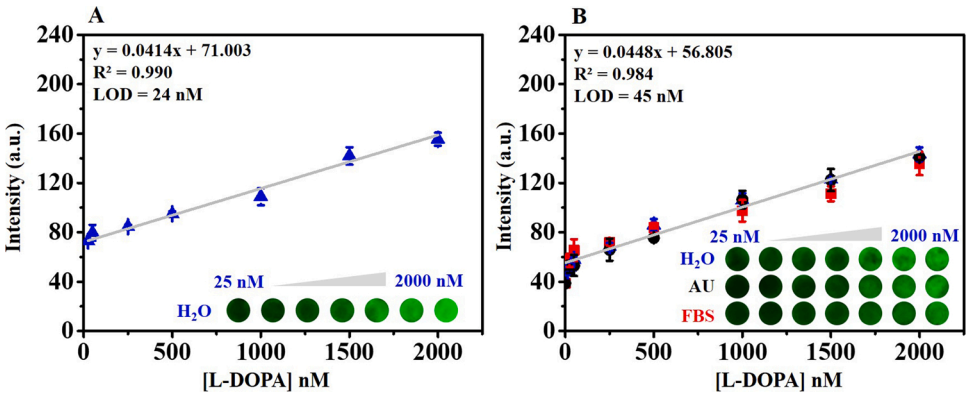

Fig. 4. (A) The green fluorescence profiles of Glu-BX molecules after mixing betalamic acid with glutamic acid for 16 h. The belalamic acid was produced in the presence of various concentrations of L-dopa (25, 50, 250, 500, 1000, 1500, and 2000 nM). Inset: the fluorescence images of ZnO-NRs papers. (B) Glu-BX molecules synthesized using cell-based methods by adding 100 μM IPTG and L-dopa at (25, 50, 250, 500, 1000, 1500, and 2000 nM), and subsequently glutamic acid in the growth media after 1 and 4 h postinduction, respectively. The linear relationships between green fluorescence and L-dopa concentrations in water, FBS, and AU were plotted. Inset: the fluorescence images of ZnO-NRs papers.

change in the surface morphology of the ZnO NRs-paper after stearic acid treatment (Fig. 2A and B). Paper treated with stearic acid concentrations of 10 or 20 mM presented a non-uniform distribution. Samples treated with 20 mM of stearic acid resulted in the increase of surface roughness (Fig. 2B), which is consistent with the results from previous study [37]. Overall, stearic acid concentrations resulted in higher contact angle; moreover, stearic acid treatment was also found to improve fluorescence intensity (approximately 27 % increase) (Fig. 2C).

3.5. Selectivity of L-dopa dioxygenase on ZnO NRs-paper

Under the optimal conditions described above, as-prepared ZnO NRs-paper samples presented a ~3-fold increase in green fluorescence compared to non-modified paper (Fig. 2C). The resulting ZnO NRs-paper samples were subsequently used to quantify L-dopa by Glu-BX green fluorescence. Selectivity for L-dopa dioxygenase was evaluated in the presence of catechol amines (DA, Epi, NE), aromatic amino acids (Phe, tyrosine, and tryptophan), and up/downstream metabolites (PEA, tyramine, and AA) at 2 μM, respectively. Green fluorescence was observed only in the presence of L-dopa regardless of the substrates, thereby demonstrating the selectivity and activity of L-dopa dioxygenase on ZnO NRs-paper (Fig. 3A). We further examined the co-presence of catecholamines. Green fluorescence intensities were compared in the solutions containing L-dopa alone, L-dopa with DA/NE/Epi, and a mixture of four. As shown in (Fig. 3B), intensities of green fluorescence remained similarly in the co-presence of catecholamines, indicating low interference from catecholamines.

3.6. Protein- and cell-based methods for quantification of L-dopa

The efficacy of as-prepared ZnO NRs-paper as an analytical tool was assessed in terms of the green fluorescence intensity of Glu-BX as an indication of L-dopa concentrations. As the concentration of L-dopa was increased from the range of 25–2000 nM, we observed a gradual increase in green fluorescence intensity. The calibration plot was linearly fitted, as follows: grayscale intensity (a.u.) = 0.0414 × [L-dopa] nM + 71.003 (a.u.) (R^2 = 0.990). The L-dopa limit of detection was 24 nM (Fig. 4A). To reduce the reaction time for imine condensation, we employed a cell-based approach to synthesizing Glu-BX. The bioproduction process of Glu-BX was carried out by taking bacterial supernatants containing Glu-BX without extra purification. This significantly reduced the reaction time from 16 to 4 h. Under these conditions, we observed a similar linear relationship between green fluorescence and the concentration of L-dopa ranging from 25 to 2000 nM and the limit of detection was 45 nM (Fig. 4B). According to Shahrokhian et al. [38], the peak plasma concentrations of L-dopa in the blood of Parkinson's disease patients on L-dopa therapy ranges from 1.26 to 12.27 μM [39,40], and the plasma level for healthy individuals is normally at 30–40 nM [41]. Thus, the as-developed assay could meet the clinical requirements for the monitoring of L-dopa in Parkinson's patients.

3.7. Measuring L-dopa in AU and FBS matrix

We also evaluated as-prepared ZnO NR-paper as an analytic tool using complex matrixes containing AU and FBS at dilution ratios of 10, 20, 30, 40 and 50 % in order to mimic real-world physiologic conditions. Overall, the green fluorescence intensity of Glu-BX was identical to those obtained under buffer conditions (Fig. S3A). When AU or FBS were spiked with various concentrations of L-dopa, the recovery range was (83–120 %) and relative standard deviation (RSD) was ≤10 % (Table S3B).

4. Conclusions

This paper outlines the fabrication and characterization of ZnO NRs-paper for the detection of L-dopa under various synthesis conditions. The ZnO NRs-paper outer performed unmodified paper samples, as indicated by a ~3-fold increase in Glu-BX green fluorescence and enhanced sensitivity in the detection of L-dopa at concentrations of the range of 25–2000 nM, with a detection limit of 24 nM. A comparison of linear ranges and LOD obtained with several enzyme and nanomaterial-based methods for the determination of L-dopa was listed in **Table S1**. Many approaches have been developed for the fast detection of L-dopa (Table S1); however, as-prepared ZnO-NRs/papers are sensitive, simple, and cost-effective alternatives to conventional analytical methods. The efficacy of the resulting paper samples was also evaluated using urine and serum samples. The proposed ZnO-NR-paper detection samples provide a convenient yet highly sensitive approach to measuring L-dopa concentrations in biofluids.

CRediT authorship contribution statement

Yu-Hsuan Lin: Data curation, Visualization, Investigation, Writing - original draft, Software, Validation. **Yi-Chun Yeh:** Conceptualization, Methodology, Writing - review & editing.

Declaration of Competing Interest

The authors declare that they have no known competing financial interests or personal relationships that could have appeared to influence the work reported in this paper.

Acknowledgments

This work was funded by the Ministry of Science and Technology of Taiwan under the project number 107-2113-M-003-013-MY3.

Appendix A. Supplementary data

Supplementary material related to this article can be found, in the online version, at doi:https://doi.org/10.1016/j.colsurfb.2021.111995.

References

[1] S. Majumdar, P. Banerji, Effect of Li incorporation on the structural and optical properties of ZnO, Superlattices Microstruct. 45 (2009) 583–589.
[2] H. Cui, Q. Liu, R. Li, X. Wei, Y. Sun, Z. Wang, L. Zhang, X.Z. Zhao, B. Hua, S.S. Guo, ZnO nanowire-integrated bio-microchips for specific capture and non-destructive release of circulating tumor cells, Nanoscale 12 (2020) 1455–1463.
[3] F. Xu, Y. Shen, L. Sun, H. Zeng, Y. Lu, Enhanced photocatalytic activity of hierarchical ZnO nanoplate-nanowire architecture as environmentally safe and facilely recyclable photocatalyst, Nanoscale 3 (2011).
[4] M. Chen, L. Hu, J. Xu, M. Liao, L. Wu, X. Fang, ZnO hollow-sphere nanofilm-based high-performance and low-cost photodetector, Small 7 (2011) 2449–2453.
[5] O. Geuli, I. Lewinstein, D. Mandler, Composition-tailoring of ZnO-Hydroxyapatite nanocomposite as bioactive and antibacterial coating, ACS Appl. Nano Mater. 2 (2019) 2946–2957.
[6] Y. Quan, J. Yao, S. Yang, L. Chen, J. Li, Y. Liu, J. Lang, H. Shen, Y. Wang, Y. Wang, J. Yang, M. Gao, ZnO nanoparticles on MoS2 microflowers for ultrasensitive SERS detection of bisphenol A, Microchimica Acta 186 (2019) 593.
[7] L. Zhang, Y. Jiang, Y. Ding, M. Povey, D. York, Investigation into the antibacterial behaviour of suspensions of ZnO nanoparticles (ZnO nanofluids), J. Nanopart. Res. 9 (2007) 479–489.
[8] F. Xie, W. Hu, D. Ning, L. Zhuo, J. Deng, Z. Lu, ZnO nanowires decoration on carbon fiber via hydrothermal synthesis for paper-based friction materials with improved friction and wear properties, Ceram. Int. 44 (2018) 4204–4210.
[9] A. Sugunan, H.C. Warad, M. Boman, J. Dutta, Zinc oxide nanowires in chemical bath on seeded substrates: role of hexamine, J. Solgel Sci. Technol. 39 (2006) 49–56.
[10] Y. Zhang, M.K. Ram, E.K. Stefanakos, D.Y. Goswami, Synthesis, characterization, and applications of ZnO nanowires, J. Nanomater. 2012 (2012).
[11] S. Tiwari, M. Vinchurkar, V.R. Rao, G. Garnier, Zinc oxide nanorods functionalized paper for protein preconcentration in biodiagnostics, Sci. Rep. 7 (2017), 43905.
[12] P.-S. Cho, K.-W. Kim, J.-H. Lee, NO_2 sensing characteristics of ZnO nanorods prepared by hydrothermal method, J. Electroceramics 17 (2006) 975–978.
[13] S. Baruah, J. Dutta, Effect of seeded substrates on hydrothermally grown ZnO nanorods, J. Solgel Sci. Technol. 50 (2009) 456–464.
[14] T. Wang, J. Costan, A. Centeno, J.S. Pang, D. Darvill, M.P. Ryan, F. Xie, Broadband enhanced fluorescence using zinc-oxide nanoflower arrays, J. Mater. Chem. C 3 (2015) 2656–2663.
[15] N. Zhang, R. Yi, R. Shi, G. Gao, G. Chen, X. Liu, Novel rose-like ZnO nanoflowers synthesized by chemical vapor deposition, Mater. Lett. 63 (2009) 496–499.
[16] J.-W. Kim, Y. Porte, K.Y. Ko, H. Kim, J.-M. Myoung, Micropatternable double-faced ZnO nanoflowers for flexible gas sensor, ACS Appl. Mater. Interfaces 9 (2017) 32876–32886.
[17] C. Yang, Y. Xu, M. Wang, T. Li, Y. Huo, C. Yang, B. Man, Multifunctional paper strip based on GO-veiled Ag nanoparticles with highly SERS sensitive and deliverable properties for high-performance molecular detection, Opt. Express 26 (2018) 10023–10037.
[18] X. Ge, A.M. Asiri, D. Du, W. Wen, S. Wang, Y. Lin, Nanomaterial-enhanced paper-based biosensors, TrAC Trends Anal. Chem. 58 (2014) 31–39.
[19] H. Tan, Q. Li, C. Ma, Y. Song, F. Xu, S. Chen, L. Wang, Lanthanide-functionalized silver nanoparticles for detection of an anthrax biomarker and test paper fabrication, J. Nanopart. Res. 16 (2014) 1–11.
[20] K.-H. Lu, J.-H. Lin, C.-Y. Lin, C.-F. Chen, Y.-C. Yeh, A fluorometric paper test for chromium(VI) based on the use of N-doped carbon dots, Microchim. Acta 186 (2019), 227.
[21] U. Gul, S. Kanwal, S. Tabassum, M.A. Gilani, A. Rahim, Microwave-assisted synthesis of carbon dots as reductant and stabilizer for silver nanoparticles with enhanced-peroxidase like activity for colorimetric determination of hydrogen peroxide and glucose, Microchim. Acta 187 (2020), 135.
[22] S. Muramatsu, K. Fujimoto, S. Kato, H. Mizukami, S. Asari, K. Ikeguchi, T. Kawakami, M. Urabe, A. Kume, T. Sato, E. Watanabe, K. Ozawa, I. Nakano, A phase I study of aromatic L-amino acid decarboxylase gene therapy for Parkinson's disease, Mol. Ther. 18 (2010) 1731–1735.
[23] S. Fahn, The medical treatment of Parkinson disease from James Parkinson to George Cotzias, Mov. Disord. 30 (2015) 4–18.
[24] E.L. Lane, L-DOPA for Parkinson's disease—a bittersweet pill, Eur. J. Neurosci. 49 (2019) 384–398.
[25] S.K. Mamta, K. Raghuveer, C.C. Sudhakumari, A. Rajakumar, Y. Basavaraju, B. Senthilkumaran, Cloning and expression analysis of tyrosine hydroxylase and changes in catecholamine levels in brain during ontogeny and after sex steroid analogues exposure in the catfish, Clarias batrachus, Gen. Comp. Endocrinol. 197 (2014) 18–25.
[26] B. Brunetti, G. Valdés-Ramírez, I. Litvan, J. Wang, A disposable electrochemical biosensor for L-DOPA determination in undiluted human serum, Electrochem. Commun. 48 (2014) 28–31.
[27] F. Bugamelli, C. Marcheselli, E. Barba, M.A. Raggi, Determination of L-dopa, carbidopa, 3-O-methyldopa and entacapone in human plasma by HPLC-ED, J. Pharm. Biomed. Anal. 54 (2011) 562–567.
[28] X. Ling, R. Shi, J. Zhang, D. Liu, M. Weng, C. Zhang, M. Lu, X. Xie, L. Huang, W. Huang, Dual-signal luminescent detection of dopamine by a single type of lanthanide-doped nanoparticles, ACS Sens. 3 (2018) 1683–1689.
[29] L. Wang, D. Su, S.N. Berry, J. Lee, Y.T. Chang, A new approach for turn-on fluorescence sensing of l-DOPA, Chem. Commun. (Cambridge, Engl.) 53 (2017) 12465–12468.
[30] X. Zheng, Y. Guo, J. Zheng, X. Zhou, Q. Li, R. Lin, Simultaneous determination of ascorbic acid, dopamine and uric acid using poly(l-leucine)/DNA composite film modified electrode, Sens. Actuators B Chem. 213 (2015) 188–194.
[31] H. Wang, Y. He, Recent advances in silicon nanomaterial-based fluorescent sensors, Sensors 17 (2017) 268.
[32] H. Singh, A. Bamrah, S.K. Bhardwaj, A. Deep, M. Khatri, K.-H. Kim, N. Bhardwaj, Nanomaterial-based fluorescent sensors for the detection of lead ions, J. Hazard. Mater. (2020), 124379.
[33] Q. Li, L. Liu, J.-W. Liu, J.-H. Jiang, R.-Q. Yu, X. Chu, Nanomaterial-based fluorescent probes for live-cell imaging, TrAC Trends Anal. Chem. 58 (2014) 130–144.
[34] Y.-C. Chou, C.-I. Shih, C.-C. Chiang, C.-H. Hsu, Y.-C. Yeh, Reagent-free DOPA-dioxygenase colorimetric biosensor for selective detection of L-DOPA, Sens. Actuators B Chem. 297 (2019).
[35] X. Guo, L. Zong, Y. Jiao, Y. Han, X. Zhang, J. Xu, L. Li, C.W. Zhang, Z. Liu, Q. Ju, J. Liu, Z. Xu, H.D. Yu, W. Huang, Signal-enhanced detection of multiplexed cardiac biomarkers by a paper-based fluorogenic immunodevice integrated with zinc oxide nanowires, Anal. Chem. 91 (2019) 9300–9307.
[36] B. Lin, Z. Fu, Y. Jia, Green luminescent center in undoped zinc oxide films deposited on silicon substrates, Appl. Phys. Lett. 79 (2001) 943–945.
[37] A.B. Gurav, S.S. Latthe, R.S. Vhatkar, J.-G. Lee, D.-Y. Kim, J.-J. Park, S.S. Yoon, Superhydrophobic surface decorated with vertical ZnO nanorods modified by stearic acid, Ceram. Int. 40 (2014) 7151–7160.
[38] S. Shahrokhian, E. Asadian, Electrochemical determination of l-dopa in the presence of ascorbic acid on the surface of the glassy carbon electrode modified by a bilayer of multi-walled carbon nanotube and poly-pyrrole doped with tiron, J. Electroanal. Chem. 636 (2009) 40–46.

[39] R.M. Riggin, R.L. Alcorn, P.T. Kissinger, Liquid chromatographic method for monitoring therapeutic concentrations of L-dopa and dopamine in serum, Clin. Chem. 22 (1976) 782–784.
[40] C. Muzzi, E. Bertocci, L. Terzuoli, B. Porcelli, I. Ciari, R. Pagani, R. Guerranti, Simultaneous determination of serum concentrations of levodopa, dopamine, 3-O-methyldopa and alpha-methyldopa by HPLC, Biomed. Pharmacother. 62 (2008) 253–258.
[41] T. Kajisa, W. Li, T. Michinobu, Catecholamine detection using a functionalized poly (l-dopa)-Coated gate field-effect transistor, ACS Omega 3 (2018) 6719–6727.